TECHNICAL REPORTS

nature neuroscience

A viral strategy for targeting and manipulating interneurons across vertebrate species

Jordane Dimidschstein[1–3], Qian Chen[4,14], Robin Tremblay[1,2,14], Stephanie L Rogers[1,2], Giuseppe-Antonio Saldi[1,2], Lihua Guo[1–3], Qing Xu[1–3], Runpeng Liu[4], Congyi Lu[4], Jianhua Chu[5,6], Joshua S Grimley[7], Anne-Rachel Krostag[7], Ajamete Kaykas[7], Michael C Avery[8], Mohammad S Rashid[8], Myungin Baek[1,2], Amanda L Jacob[9], Gordon B Smith[9], Daniel E Wilson[9], Georg Kosche[1,10], Illya Kruglikov[11], Tomasz Rusielewicz[11], Vibhakar C Kotak[12], Todd M Mowery[12], Stewart A Anderson[5,6], Edward M Callaway[8], Jeremy S Dasen[1,2], David Fitzpatrick[9], Valentina Fossati[11], Michael A Long[1,10], Scott Noggle[11], John H Reynolds[8], Dan H Sanes[12], Bernardo Rudy[1,2], Guoping Feng[4,13] & Gord Fishell[1–3]

A fundamental impediment to understanding the brain is the availability of inexpensive and robust methods for targeting and manipulating specific neuronal populations. The need to overcome this barrier is pressing because there are considerable anatomical, physiological, cognitive and behavioral differences between mice and higher mammalian species in which it is difficult to specifically target and manipulate genetically defined functional cell types. In particular, it is unclear the degree to which insights from mouse models can shed light on the neural mechanisms that mediate cognitive functions in higher species, including humans. Here we describe a novel recombinant adeno-associated virus that restricts gene expression to GABAergic interneurons within the telencephalon. We demonstrate that the viral expression is specific and robust, allowing for morphological visualization, activity monitoring and functional manipulation of interneurons in both mice and non-genetically tractable species, thus opening the possibility to study GABAergic function in virtually any vertebrate species.

Inhibitory GABAergic interneurons, although sparser in number than glutamatergic neurons, play critical roles in all central processing, and their dysfunction contributes to numerous neuropsychiatric disorders[1–3]. To date, the ability to target interneurons has been essentially limited to the use of transgenic mice[4]. While certain cell types, such as principal excitatory cells and glia, have been successfully targeted[5–7], an effective approach to target inhibitory interneurons is not currently available. Gene delivery using nonpathogenic recombinant adeno-associated virus (rAAV) is showing increasing promise for the treatment of both monoallelic and complex diseases. Many phase I–III clinical trials using rAAV vectors have yielded encouraging results, and in 2012, the first rAAV-based therapy received marketing approval from the European Union[8]. Despite its promise, the use of AAV as a gene-delivery method is hampered by its limited selectivity in expression. While it has been long recognized that including *cis*-acting DNA control elements[9–14], such as specific promoters or enhancers, within rAAVs might provide the desired specificity for expression within particular target cells in the brain, the success of such strategies has been limited. With regard to rAAVs, the chief obstacle to this approach is the fundamental incompatibility of the size of such control elements relative to the restricted packaging limit of AAVs[15,16]. Given the obligate minimal size of reporters (for example, EGFP or dTomato) alone or in combination with effector elements (for example, ChR2 or DREADD), which average about 700 bp to 2 kb, respectively, a maximum of ~2 kb in packaging capacity remains for the insertion of a *cis*-acting DNA control element into the viral vector. In order to identify sufficiently small elements capable of restricting expression to a defined population of cells, we examined regulatory elements known in other contexts to be specific to interneurons[17–19]. The distalless homeobox 5 and 6 (*Dlx5/6*) genes are specifically expressed by all forebrain GABAergic interneurons during embryonic development. These genes have an inverted orientation relative to one another and share a 400 bp (*mI56i* or mDlx) and a 300 bp (*mI56ii*) enhancer sequence in the 10 kb noncoding intergenic region 3′ to each of them[17,20]. The high degree of conservation of these sequences across vertebrate species is suggestive of an important

[1]NYU Neuroscience Institute, New York University Langone Medical Center, New York, New York, USA. [2]Department of Neuroscience and Physiology, Smilow Research Center, New York University Langone Medical Center, New York, New York, USA. [3]Center for Genomics & Systems Biology, New York University, Abu Dhabi, UAE. [4]McGovern Institute for Brain Research, Department of Brain and Cognitive Sciences, Massachusetts Institute of Technology, Cambridge, Massachusetts, USA. [5]Department of Psychiatry, Children's Hospital of Philadelphia, Philadelphia, Pennsylvania, USA. [6]Perelman School of Medicine, University of Pennsylvania, Philadelphia, Pennsylvania, USA. [7]Allen Institute for Brain Science, Seattle, Washington, USA. [8]Systems Neurobiology Laboratories, Salk Institute for Biological Studies, La Jolla, California, USA. [9]Department of Functional Architecture and Development of Cerebral Cortex, Max Planck Florida Institute for Neuroscience, Jupiter, Florida, USA. [10]Department of Otolaryngology, Smilow Research Center, New York University Langone Medical Center, New York, New York, USA. [11]New York Stem Cell Foundation, New York, New York, USA. [12]NYU Center for Neural Science, New York University, New York, New York, USA. [13]Stanley Center for Psychiatric Research, Broad Institute of MIT and Harvard, Cambridge, Massachusetts, USA. [14]These authors contributed equally to this work. Correspondence should be addressed to G.F. (gordon.fishell@med.nyu.edu).

Received 9 May; accepted 27 September; published online 31 October 2016; corrected after print 29 November 2016; addendum published after print 29 May 2017; doi:10.1038/nn.4430

role in gene regulation. Indeed, the mDlx enhancer has been used in numerous contexts to reliably target reporter genes in a pattern very similar to the normal patterns of *Dlx5/6* expression during embryonic development[17,21–24].

RESULTS

The mDlx enhancer restricts reporter expression to GABAergic interneurons *in vitro*

We first aimed to determine whether the mDlx enhancer can restrict the expression of reporter genes to GABAergic interneuron *in vitro* using rAAV. We inserted the mDlx enhancer in front of a minimal promoter in an AAV backbone, using the genetically encoded calcium indicator GCaMP6f construct as a reporter to monitor expression (rAAV-mDlx-GCaMP6f). Primary cortical neuronal cultures from mice were infected with rAAV-mDlx-GCaMP6f, cultured for 11 d after infection and examined for GCaMP6f expression. We observed that the majority of cells that expressed GCaMP6f also expressed the pan-interneuron marker Gad67 (~95%; **Fig. 1a**,**i**). As expected, expression of GCaMP6f driven by an rAAV containing a promoter that targets excitatory neurons (CaMK2a) was excluded from GABAergic interneurons (**Supplementary Fig. 1a**). To test whether the level of GCaMP6f expression in interneurons was sufficient to allow their activity to be monitored, we performed *in vitro* calcium imaging. Consistent with their high level of expression, robust spontaneous calcium transients could be detected in primary culture of cortical neurons *in vitro* (**Supplementary Fig. 1b**). Taken together, these data demonstrate that the mDlx enhancer alone was sufficient both to restrict the expression of a reporter to interneurons and to allow monitoring of neuronal activity of interneurons *in vitro* when used to direct GCaMP6f expression.

The mDlx enhancer restricts reporter expression to adult GABAergic interneurons in the forebrain

A number of aspects of *Dlx5/6* gene expression compromise their utility as markers for interneurons. *Dlx5/6* genes are highly expressed in progenitors of GABAergic and postmitotic interneurons during embryonic development, but their expression strongly diminishes after birth. Moreover, in the striatum these genes are not specific to interneurons, as both interneurons and medium spiny neurons (4% and 96% of the population, respectively; medium spiny neurons are the principal projection neurons) express high levels of *Dlx5/6* during embryonic development[17,18,25]. Groups that have used the mDlx enhancer in transgenic mice have found that reporters under the control of this element are faithfully expressed in a pattern that closely matches endogenous patterns of *Dlx5/6* expression, demonstrating the unsuitableness of using this approach to either label interneurons postnatally or to differentiate between interneurons and medium spiny neurons within the striatum[17,21–24]. This prompted us to test whether rAAV-mDlx-GFP virus had similar limitations in its ability to target interneuronal populations. Unexpectedly, immunofluorescence analyses of adult mice 1 week after injection with rAAV-mDlx-GFP revealed sparse but strong GFP labeling in somatosensory cortex (S1), hippocampus and striatum (**Fig. 1b**), indicative of the labeling of interneurons. To confirm the identity of these cells, we injected rAAV-mDlx-GFP into the cortex and hippocampus of *Dlx6aCre:Ai9* mice, where the persistence of the RFP reporters subsequent to the cessation of *Dlx6* expression results in all interneurons within these areas being RFP-positive. Again, the majority of GFP-expressing cells coexpressed RFP (**Fig. 1c**,**d**,**j**). Moreover, rAAV-mDlx-GFP expression within the striatum colocalized with Nkx2.1, an interneuron marker within this structure (**Fig. 1e**,**k**). Consistent with the expression of GFP being uniformly observed within all interneuron populations, within S1, the infected cells expressed parvalbumin, somatostatin and vasoactive intestinal peptide (VIP) in proportions that corresponded to the expected layer distribution of these three non-overlapping interneuron markers in this region[1,26] (**Fig. 1f–h**,**i**). To investigate whether the mDlx enhancer could also drive expression in interneurons not derived from the *Dlx5/6* lineage, we performed viral injections in the lumbar region of the spinal cord of postnatal day 0 pups and analyzed the expression of the viral reporter after 7 d. In mice injected with rAAV-mDlx-GFP, the GFP expression appeared to be restricted to the dorsal horns of the lumbar spinal cord, and virtually no cells expressing the viral reporter colocalized with Pax2, a marker exclusively expressed in virtually all GABAergic and glycinergic interneurons of the dorsal horns of the spinal cord in both embryonic and adult animals[27]. By contrast, mice injected with an AAV expressing nuclear GFP under the control of the pan-neuronal promoter human synapsin1 (rAAV-hSyn1-nGFP) showed widespread expression of GFP within both ventral and dorsal spinal cord, with ~12% of cells colocalizing with Pax2 (**Supplementary Fig. 2**). These data show that the expression driven by the mDlx enhancer was excluded from the inhibitory neurons in the spinal cord, but restricted to a population of cells in the dorsal spinal cord that remains to be characterized. Altogether, these results demonstrate that infection of adult mice with rAAV-mDlx-GFP resulted in a highly selective expression within GABAergic interneurons from the *Dlx5/6* lineage within the telencephalon.

rAAV-mDlx-Flex-GFP allows for the intersectional targeting of interneuron subtypes

Despite significant progress in recent years, the precise targeting and manipulation of specific interneuron subtypes is still essentially limited to the combinatorial use of transgenic mice expressing Cre and Flp recombinases in defined populations[4,28]. The specificity of targeting is thus hampered by the availability of driver lines and the time-consuming breeding associated with generating productive crosses on suitable genetic backgrounds. Therefore, we asked whether the specificity of the rAAV-Dlx for interneurons could be leveraged to develop an intersectional strategy that would require only one Cre-expressing mouse reporter. To test this idea, we injected an rAAV that expressed a Cre-dependent GFP reporter under the control of the mDlx enhancer (rAAV-mDlx-Flex-GFP) into *Cck-Cre* transgenic mice. While *Cck* is expressed in specific subsets of interneurons, its broader expression within glutamatergic neurons limits the usefulness of *Cck-Cre* mice for targeting interneurons[4]. In both somatosensory cortex S1 and hippocampal CA1, the majority of cells expressing GFP coexpressed the pan-interneuron marker Gad67 (**Fig. 2**). Importantly, *Cck-Cre* mice injected with an rAAV that expressed a Cre-dependent GFP reporter under the control of an ubiquitous promoter (rAAV-CAG-Flex-GFP) showed that the GFP expression was not selective for interneurons, and animals that do not express Cre-recombinase injected with rAAV-mDlx-Flex-GFP did not show GFP expression at the injection site (**Supplementary Fig. 3**). These data demonstrate that the mDlx enhancer restricted the expression of a recombinase-dependent reporter to interneurons and can be used as a simplified intersectional strategy. Importantly, to test whether Cre-recombinase itself can be selectively directed by this approach, we injected an rAAV that expressed nuclear dTomato and Cre or destabilized Cre under the control of the mDlx enhancer (rAAV-mDlx-Cre or rAAV-mDlx-dCre) into *RCE-loxP* transgenic mice. While dTomato was confined to the interneuron population, in animals injected with Cre and dCre virtually all cells expressed GFP at the injection site (data not shown).

This demonstrates that trace amounts of Cre-recombinase were sufficient to drive expression of a Cre-dependent genetic reporter and thus suggests that specificity of expression of recombinases cannot be achieved using this approach.

rAAV-hDLX-Gq-DREADD allows for chemogenetic modulation of interneuronal activity

Having established that our strategy enabled high expression of fluorescent reporters (GFP) and activity indicators (GCaMP6f) restricted to interneurons, we next sought to examine whether chemogenetic approaches could be used to manipulate interneuron activity. Designer receptors exclusively activated by designer drugs (DREADDs) are modified human muscarinic receptors that are activated by clozapine-N4-oxide (CNO), a pharmacologically inert and orally bioavailable drug[29]. To date, their utilization in interneurons has been restricted to contexts involving the use of transgenic mice[30–33]. To test whether we could use rAAV-hDlx to gain chemogenetic control of interneurons, we generated an rAAV-hDlx-Gq expressing a hemagglutinin

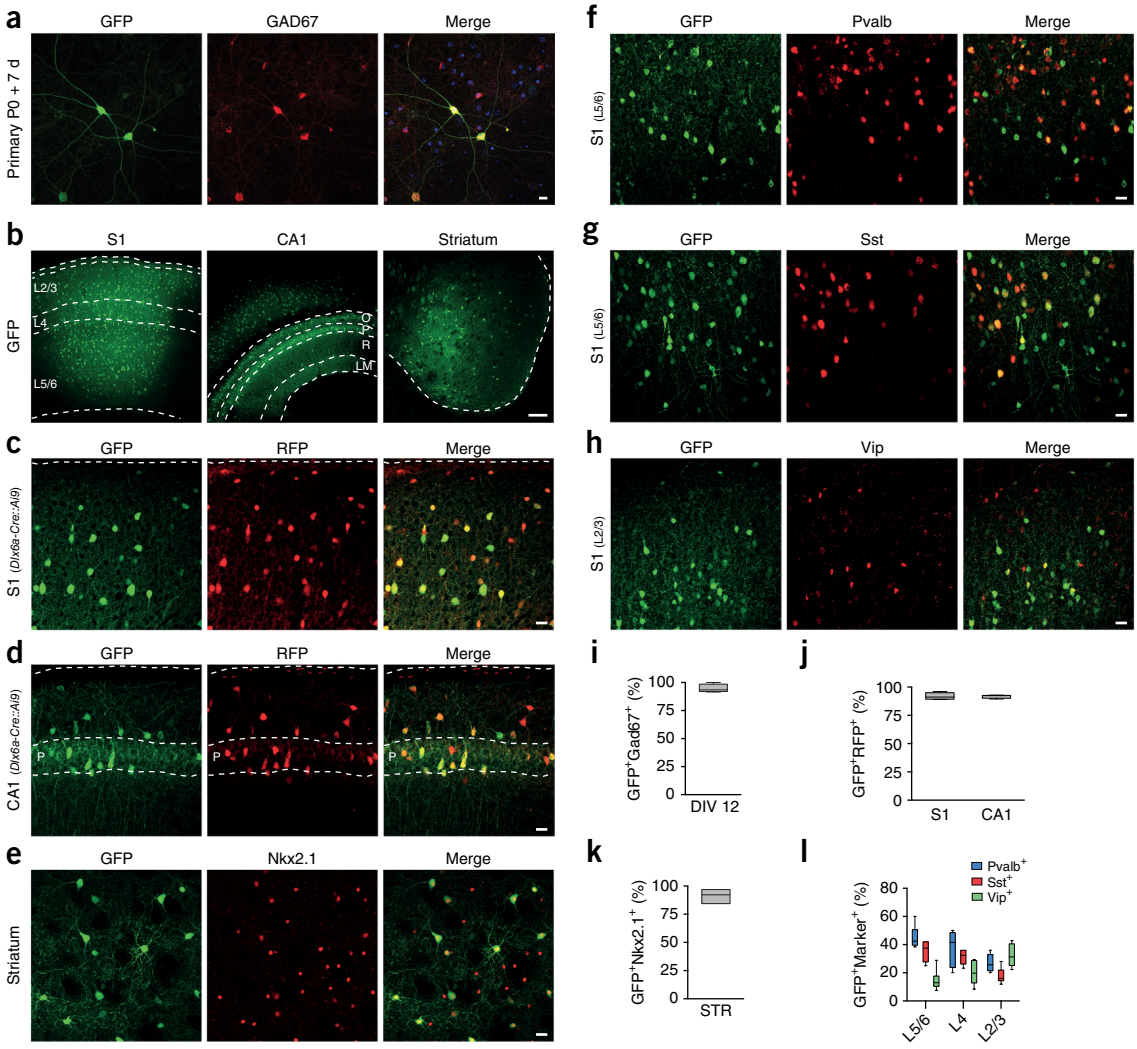

Figure 1 rAAV with mDlx enhancer restricts reporter expression to GABAergic interneurons. (**a**) Postnatal day (P) 0 primary cortical cultures were infected with rAAV-mDlx-GCaMP6f at 8 days *in vitro* (DIV) and analyzed at DIV 19 by immunostaining using GFP and Gad67 antibodies. Representative example of colocalization between GFP and Gad67 (quantitation of this is shown in **i**). (**b**–**h**) Adult C57Bl6 ($n = 16$) or *Dlx6aCre::Ai9* ($n = 4$) mice were stereotactically injected with 50–100 nl of rAAV-mDlx-GFP in the indicated brain regions and were analyzed by immunostaining for the indicated markers after 7 d. Representative examples of GFP expression and colocalization between GFP and the indicated marker. (**i**) Quantitation of colocalization of rAAV-mediated viral expression of GFP and Gad67 in DIV 19 cultured cortical neurons (94.7 ± 1.8%, $n = 875$ cells from 5 coverslips). (**j**–**l**) Quantification of the proportion of cells coexpressing GFP and the indicated marker in the indicated anatomical regions. GFP^+RFP^+: *Dlx6a-Cre::Ai9*, S1: 92.8 ± 1.2%, $n = 657$ cells from 4 animals; GFP^+RFP^+: *Dlx6a-Cre::Ai9*, CA1: 91.8 ± 0.9%, $n = 210$ cells from 4 animals; $GFP^+Nkx2.1^+$: C57Bl6, in striatum: 36.4 ± 2.6%, $n = 284$ cells from 3 animals; GFP^+Pvalb^+: C57Bl6, in S1: layer (L) 2/3: 26.9 ± 2.5%; in L4: 37.7 ± 5.1%; in L5/6: 45.1 ± 3.2%; total $n = 577$ from 3 animals; GFP^+Sst^+: C57Bl6, in S1: in L2/3: 17.8 ± 2.3%; in L4: 32.3 ± 1.6%; in L5/6: 35.4 ± 3.0%; total $n = 577$ from 3 animals; GFP^+VIP^+: C57Bl6, in S1: in L2/3: 32.6 ± 3.3%; in L4: 20.0 ± 3.4%; in L5/6: 14.6 ± 3.0%; total $n = 701$ from 4 animals. Quantification are indicated in the text as mean ± s.e.m. and are represented as box-and-whisker plot with upper and lower whiskers representing the maximum and minimum value respectively while the boxes represent upper, median and lower quartiles. Dashed lines in **b** and **d** represent limits of the indicated anatomical structures. Roman numbers represent cortical layers: O, oriens; P, pyramidal; R, radiatum; LM, lacunosum moleculare. Scale bars represent 10 µm (in **a**), 15 µm (in **c**–**h**) or 100 µm (in **b**). S1, somatosensory cortex; CA1, hippocampus; Pvalb, parvalbumin; Sst, somatostatin; VIP, vasoactive intestinal peptide.

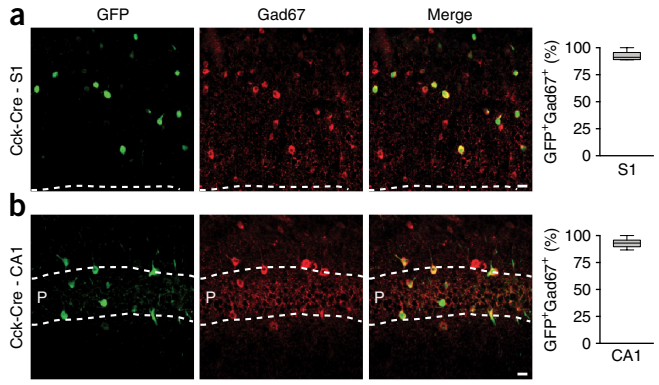

Figure 2 rAAV-mDlx-Flex-GFP allows intersectional targeting of Cck-expressing interneurons. Adult *Cck-Cre* mice ($n = 4$) were injected with rAAV-mDlx-Flex-GFP in somatosensory cortex (S1) or hippocampus (CA1) and were analyzed after 2 weeks by immunostaining for Gad67 immunoreactivity after 2 weeks. (**a**,**b**) Representative example of colocalization between GFP and Gad67 and corresponding quantifications (S1: 92.4 ± 1.4%, $n = 319$ cells from 4 animals; CA1: 93.2 ± 1.1%, $n = 219$ cells from 4 animals). Quantification are indicated as mean ± s.e.m. and are represented as box-and-whisker plot with upper and lower whiskers representing the maximum and minimum values, respectively, and the boxes representing upper, median and lower quartiles. Dashed lines represent limits of indicated anatomical structures. Scale bars, 10 µm.

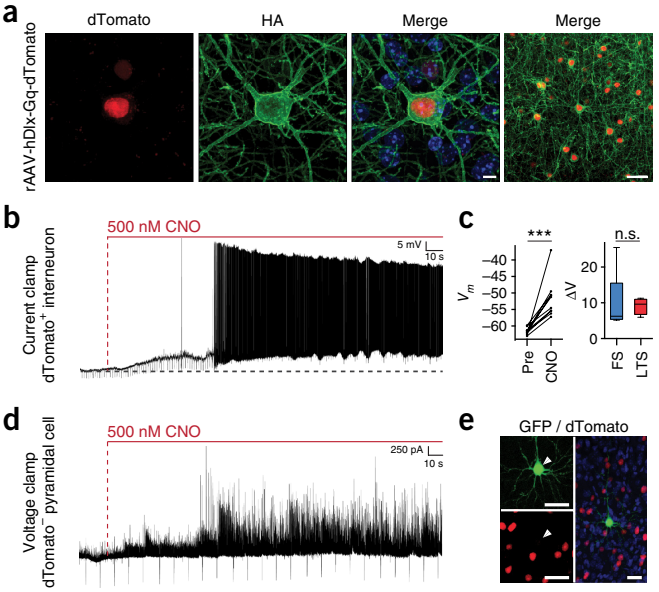

Figure 3 rAAV-hDLX-Gq-DREADD allows chemogenetic modulation of interneuronal activity in mice. Adult C57Bl6 mice ($n = 18$) were stereotactically injected with rAAV-hDlx-HA-Gq-DREADD-P2A-NLS-dTomato in somatosensory cortex and were either analyzed by immunostaining for the indicated markers after 7 d or sectioned for electrophysiological recording after 4 weeks. (**a**) Representative example of colocalization between dTomato and HA-tagged Gq-DREADD in somatosensory cortex layer VI. Note the membrane localization of the Gq-DREADD. (**b**) Effect of CNO on membrane potential and firing measured in current clamp configuration of a LTS interneuron. Horizontal dashed line indicates baseline membrane potential (–60 mV). (**c**) Left: population data for effect of CNO on membrane potential. Average membrane potential (for a period of 25 s) 30 min before and 2 min after CNO exposure for individual cells ($n = 10$ cells, $P = 0.8161$; two-tailed *t*-test). Right: change in membrane potential for fast-spiking cells (FS; 10.2 ± 3.2 mV, $n = 6$ cells) and low-threshold-spiking cells (LTS; 9.6 ± 0.7 mV, $n = 4$ cells). Two-tailed *t*-test, $P < 0.001$. (**d**) Effect of CNO on inhibitory drive measured in voltage clamp configuration from a whole-cell recording of a pyramidal neuron within the area of viral infection. (**e**) *Post hoc* immunostaining of a biocytin-filled pyramidal neuron within the site of viral injection surrounded by interneurons infected by rAAV-hDlx-HA-Gq-DREADD-P2A-NLS-dTomato. Nuclei were counterstained with DAPI (blue). Arrowheads point to the recorded cell. Unpaired *t*-test: $***P < 0.001$; n.s., nonsignificant. Quantification are indicated as mean ± s.e.m. and represented as box-and-whisker plots with upper and lower whiskers representing the maximum and minimum values, respectively, and the boxes representing upper, median and lower quartiles. Vertical dashed lines in indicate CNO entry in the bath. Scale bars, 5 µm (**a**, left panels) or 20 µm (**a**, right panel and **e**).

(HA)-tagged version of the Gq-DREADD followed by the nuclear red-fluorescent reporter NLS-dTomato, under the control of the humanized form of the Dlx enhancer element (**Supplementary Fig. 4a**). We first tested whether the use of the human form of the *Dlx5/6* enhancer (hDlx) negatively impacted the targeting specificity of the virus. Immunofluorescence analyses of adult *Dlx6aCre::RCE* mice (where GFP expression in the cortex and hippocampus was restricted to interneurons) injected with rAAV-hDlx-Gq in S1 and CA1 revealed that the majority of cells expressing dTomato also expressed GFP **Supplementary Fig. 4b–d**). In addition, consistent with the expected expression of a functional receptor, the Gq-DREADD was located at the membrane of the infected cells (**Fig. 3a** and **Supplementary Fig. 4e**). These data confirm that rAAV-hDlx-Gq drove the expression of the Gq-DREADD exclusively within interneurons. We then formally tested the functionality of the Gq-DREADD within these cells. Upon bath application of CNO, all interneurons expressing Gq-DREADD showed membrane potential depolarization in less than 1 min, consistent with the expression of a functional receptor (**Fig. 3b**,**c**). Finally, voltage clamp recordings of a pyramidal cell in the vicinity of the Gq-DREADD-expressing interneurons showed an increase in inhibitory postsynaptic currents (iPSCs) upon CNO application (**Fig. 3d**,**e**). These experiments demonstrate that rAAV-mDlx-Gq allowed functional and restricted expression of Gq-DREADD and that CNO treatment effectively and selectively increased the activity of interneurons, allowing localized and pronounced increases in inhibitory tone within neighboring excitatory neurons.

rAAV-mDlx is selectively expressed within GABAergic interneurons in a wide variety of vertebrate species

The high degree of conservation of the mDlx enhancer sequence across vertebrates suggests a conserved role in the transcriptional regulation of the *Dlx5/6* genes[20]. We thus sought to test whether the use of rAAV-Dlx could be extended to direct the expression of a variety of different reporters and effectors, specifically in interneurons in non-genetically tractable species. This proved successful, as we were able to achieve both comparable levels and the fidelity of expression of rAAV-Dlx in neurons from five different species. Similarly to what has been observed in mice, the expression of GFP or RFP in zebra finches, ferrets, gerbils and marmosets infected with rAAV-Dlx colocalized with cells expressing the pan-interneuron markers GABA or Gad67 (**Fig. 4a–d**). Most relevant to humans, infection of neurons obtained from patient-derived induced pluripotent stem cells with rAAV-mDlx-GFP showed that the majority of the cells expressing GFP coexpressed GABA (**Fig. 5a**). To confirm these findings, we introduced rAAV-hDlx-dTomato into a coculture containing both dorsalized human embryonic stem cells (hESCs; mainly glutamatergic neurons), as well as a transgenic hESC reporter line expressing Citrine specifically in

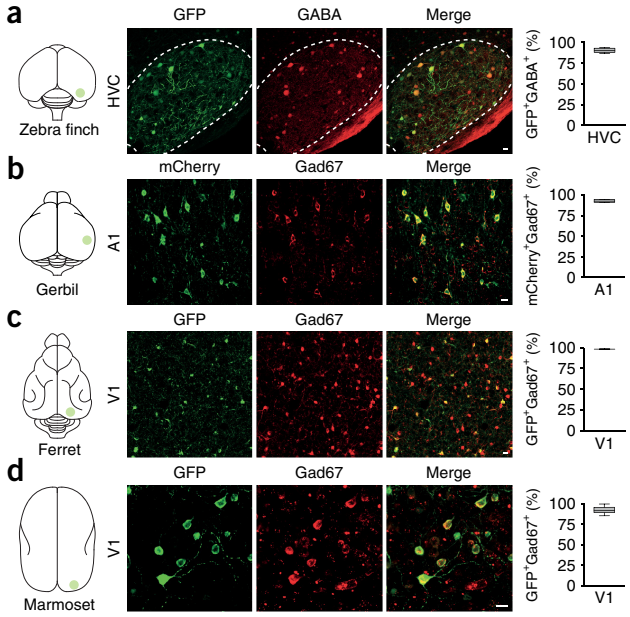

Figure 4 rAAV-mDlx is selectively expressed within GABAergic interneurons in various non-genetic model organisms. (**a**) Adult zebra finches ($n = 6$) were injected with rAAV-mDlx-GFP in high vocal center (HVC) and analyzed by immunostaining for GABA immunoreactivity after 2–4 weeks. Representative example of colocalization between GFP and GABA and corresponding quantification (90.6 ± 1.1%, $n = 104$ cells, 4 animals). (**b**) Adult gerbils ($n = 4$) were injected with rAAV-mDlx-ChR2-mCherry in V1 and analyzed by immunostaining for Gad67 immunoreactivity after 2–4 weeks. Representative example of colocalization between mCherry and Gad67 and corresponding quantification (94.0 ± 0.3%, $n = 318$ cells, 4 sections from 1 animal). (**c**) Juvenile ferrets ($n = 4$) were injected with rAAV-mDlx-GCaMP6f in V1 and analyzed by immunostaining for Gad67 immunoreactivity after 2 weeks. Representative example of colocalization between GFP and Gad67 and corresponding quantification (98.2 ± 0.5%, $n = 1{,}647$ cells, 2 animals). (**d**) An adult marmoset ($n = 1$) was injected with rAAV-mDlx-GFP in V1 and analyzed by immunostaining for Gad67 immunoreactivity after 3 months. Representative example of colocalization between GFP and Gad67 and corresponding quantification (92.6 ± 1.2%, $n = 215$ cells, 3 sections from 1 animal). Quantification are indicated as mean ± s.e.m. and are represented as box-and-whisker plots with upper and lower whiskers representing the maximum and minimum values, respectively, and the boxes represent upper, median and lower quartiles. Dashed lines represent limits of the indicated anatomical structures. Scale bars, 10 µm.

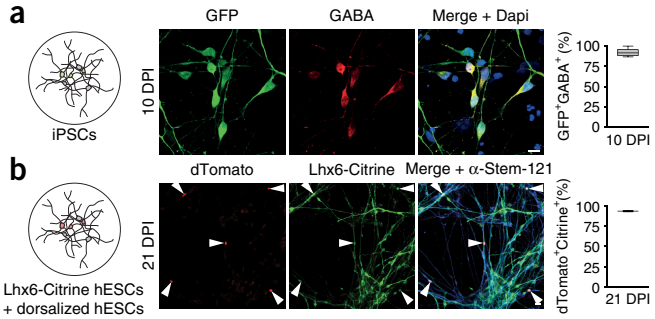

Figure 5 rAAV-Dlx restricts expression to interneurons derived from iPSCs and human embryonic stem cells. (**a**) Neuronal cultures derived from human iPSCs were inoculated with rAAV-mDlx-GFP at DIV 50 and analyzed by immunostaining for GABA immunoreactivity 10 d after inoculation (10 DPI). Representative example of colocalization between GFP and GABA and corresponding quantification (92.3 ± 1.3%, $n = 307$ cells, 6 coverslips from 2 independent experiments). (**b**) Coculture of excitatory neurons derived from hESCs and GABAergic interneurons derived from a transgenic hESC line expressing Citrine under the control of an Lhx6 promoter, inoculated with rAAV-hDlx-Gq-DREADD at DIV 1 of coculture. Cells expressing dTomato were analyzed by immunostaining for Citrine and α-Stem-121 immunoreactivity 21 DPI. Representative example of colocalization between dTomato and Citrine and corresponding quantification (93.6 ± 0.3%, $n = 128$ cells, 2 coverslips from 2 independent experiments). Quantification are indicated as mean ± s.e.m. and represented as box-and-whisker plots with upper and lower whiskers representing the maximum and minimum values, respectively, and the boxes representing upper, median and lower quartiles. White arrowheads, cells expressing dTomato. Scale bar, 10 µm (in **a**) or 20 µm (in **b**).

interneurons derived from the medial ganglionic eminence (hESC-Lhx6-Citrine). Immunostaining analysis showed that the majority of cells expressing the nuclear dTomato also expressed Citrine, while none of the dorsalized hESCs expressed dTomato (**Fig. 5b**). These results show that the Dlx enhancer restricted rAAV-mediated gene expression to interneurons in all vertebrate species tested, including human. In addition, slice and *in vivo* recordings from zebra finches injected with rAAV-mDlx-GFP showed that the GFP-expressing cells exhibited electrophysiological and morphological properties characteristic of interneurons (**Supplementary Fig. 5**). The success of this approach further highlights the potential of rAAV-Dlx for identifying and characterizing interneuron subtypes in non-genetically tractable animal models. Using *in vitro* slice recordings from gerbils injected with rAAV-mDlx-ChR2-mCherry in the auditory cortex (A1), we showed that 1-ms pulses of blue light elicited action potentials in cells expressing mCherry (**Supplementary Fig. 6a**,**b**). As expected, voltage-clamp recording of noninfected cells in the vicinity of the injection site showed an abrupt interruption of action potentials upon light activation (**Supplementary Fig. 6c**,**d**). rAAV-mDlx-ChR2-mCherry thus allows local optogenetic control of interneurons. *In vivo* calcium imaging of ferret visual cortex injected with rAAV-mDlx-GCaMP6f showed activation of interneurons upon presentation of visual stimuli (**Supplementary Fig. 7**). This demonstrated that it is possible to use this tool to monitor the functional activity of neurons in the living brain while presenting behaviorally relevant stimuli to the animal.

DISCUSSION

Transgenic approaches in mice have revolutionized our understanding of circuits. However, it is presently impossible to efficiently and reliably identify and manipulate specific neuronal subtypes in non-genetically tractable species. Here we report a new approach that directly address this challenge. rAAVs have been previously used as a safe and effective gene delivery method by researchers and clinicians in numerous contexts, but their use has been hampered by the limited cell-type selectivity that can be achieved by natural or engineered tropism[8]. Another major limitation of rAAVs is their naturally limited DNA payload (~4.7 kb). This has reduced the range of regulatory sequences that can be used to achieve cellular specific expression[15]. One way to circumvent this limitation is to use short *cis*-regulatory sequences that can regulate gene expression. Enhancers are *cis*-acting elements composed of transcription factor binding sites that are responsible for tissue-specific transcriptional regulation of gene expression. Several laboratories have taken advantage of the high degree of conservation of noncoding genomic sequences to identify putative enhancers with conserved activity between mice and humans[19,34]. The mouse *Dlx5/6* enhancer is composed of a core sequence of 297 nucleotides showing

98% identity with human and 75% identity with zebrafish; it has been extensively used to drive gene expression exclusively in interneurons in various contexts[17,21–24]. An unexpected finding from this work is the differential activity of the mDlx or hDlx enhancers when used in transgenic contexts versus rAAV contexts. While the enhancer used in the context of rAAVs continues to direct interneuron expression in adult mice, it fails to do so endogenously or in transgenic animals. It seems likely that a combination of transcription factors cooperates to direct the expression of *Dlx5/6* during embryonic development. The loss of *Dlx5/6* expression in adults is most likely either a result of a decrease in expression level of the transcription factors that bind and activate the mDlx enhancer or a result of the enhancer itself being epigenetically silenced postnatally. Either possibility is tenable, as the virus may escape epigenetic silencing by being episomal, or the large number of rAAV virions might be able to overcome reductions in transcription factor expression, such that rAAV expression can persist reliably in adults. Finally, in areas other than the telencephalon, this virus showed reliable expression, albeit in populations other than those expressing GABA. This likely reflects the presence within these cells of transcription factors able to specifically bind and activate the *Dlx5/6* enhancer and opens the possibility to explore these cellular populations in the future.

Questions of how the Dlx enhancer functions aside, our approach provides a toolbox for studying inhibitory GABAergic function across species in hippocampus, cortex and striatum and has strong potential for utility in clinical intervention. In particular, we showed that administration of CNO, the ligand for Gq-DREADD, selectively increased the activity of interneurons, resulting in an increase of local inhibition on neighboring excitatory pyramidal neurons. In mice, the use of optogenetic closed-loop recruitment of interneurons has proven effective for ameliorating seizures[35]. It has also been recently shown that reducing excitatory drive in pyramidal cells using Gi-DREADD can reduce the severity of seizures in mouse models of focal epilepsy[36]. The combination of the selectivity of rAAV-hDlx with the time control of Gq-DREADD thus allows for locally increasing the inhibitory drive of interneurons and could thus be beneficial to restore the excitatory–inhibitory balance in patients with intractable focal epilepsy.

Our results demonstrate that the mDlx enhancer can be used in the context of rAAVs to broadly and specifically target and manipulate interneurons from the *Dlx5/6* lineage. Our success in targeting these interneurons in mice, zebra finches, ferrets, gerbils and marmosets, as well as in both human iPSC-derived and ESC-derived interneurons, illustrates the potential of this approach for extending our understanding of interneuron function across a broad range of species. This raises the question of whether this approach can be generalized to target additional neuronal populations. Other enhancers with a similar degree of conservation have been already been identified[34], suggesting this might be possible. In addition, the emergence of high-throughput screening methods allowing genome-wide mapping of enhancers based on chromatin configuration and epigenetic marks has led to the discovery of many others[19,37]. It is tempting to speculate that systematic screening of sequences for their ability to direct expression in specific cell types may provide an approach for the development of novel viral tools to target and manipulate individual functional cell types with unprecedented specificity.

METHODS

Methods, including statements of data availability and any associated accession codes and references, are available in the online version of the paper.

Accession codes. Addgene: pAAV-mDlx-GFP, 83900; pAAV-mDlx-GCaMP6f, 83899; pAAV-mDlx-ChR2-mCherry, 83898; pAAV-hDlx-Gq-DREADD-dTomato, 83897; and pAAV-hDlx-Flex-GFP, 83895.

ACKNOWLEDGMENTS

We thank S. Gerard, L. Sjulson and T. Petros for discussions and comments on the manuscript. Plasmids AAV-CaMKIIa-GCaMP6f-P2A-nls-dTomato and AAV-hSyn1-GCaMP6s-P2A-nls-dTomato were a gift from J. Ting (Allen Institute for Brain Science). Plasmid pNeuroD-Ires-GFP was a gift from F. Polleux (Department of Neuroscience, Mortimer B. Zuckerman Mind Brain Behavior Institute, Columbia University Medical Center). Plasmid pGP-CMV-GCaMP6f was a gift from D. Kim (Janelia Research Campus, Howard Hughes Medical Institute). Plasmid pAAV-Ef1a-DIO hChR2(E123T/T159C)-EYFP was a gift from K. Deisseroth (Department of Bioengineering, Stanford University). Plasmid pAAV-hSyn-DIO-hM3D(Gq)-mCherry was a gift from B. Roth (Department of Pharmacology, UNC Chapel Hill Medical School).This work was supported by grants from the National Institutes of Health (NIH): MH071679, NS08297, NS074972, MH095147, as well as support from the Simons Foundation (SFARI) (to G.F.); MH066912 (to S.S.A.); and EY022577 and MH063912 (to E.M.C.).

AUTHOR CONTRIBUTIONS

J.D. conceived and designed the viral constructs, designed and performed experiments, analyzed data, prepared figures and wrote the manuscript. Q.C., C.L. and R.L. performed experiments, analyzed data and prepared figures related to mouse primary cultures. R.T. performed the slice recording experiments, analyzed the data and prepared the associated figures and text. G.-A.S. and S.L.R. performed viral injections and IHC on mice. Q.X. and L.G. produced the viruses at NYUAD using plasmids conceived and generated at NYU. G.K. performed experiments related to zebra finches. A.L.J., G.B.S. and D.E.W. performed experiments related to ferrets. V.C.K. and T.M.M. performed experiments related to gerbils. J.H.R., M.C.A. and M.S.R. performed experiments related to marmosets. I.K. and T.R. performed experiments related to iPSCs. J.C., S.A., J.S.G., A.-R.K. and A.K. performed experiments related to hESCs, M.B. and J.S.D. performed experiments related to spinal cord. S.A.A., E.M.C., D.J.S., D.F., V.F., M.A.L., S.N., J.H.R., D.H.S., B.R. and G. Feng helped with the study design. G. Fishell helped with study design, manuscript and figure preparation and supervised the project. All authors edited and approved the manuscript.

COMPETING FINANCIAL INTERESTS

The authors declare competing financial interests: details are available in the online version of the paper.

1. Rudy, B., Fishell, G., Lee, S. & Hjerling-Leffler, J. Three groups of interneurons account for nearly 100% of neocortical GABAergic neurons. *Dev. Neurobiol.* **71**, 45–61 (2011).
2. Marín, O. Interneuron dysfunction in psychiatric disorders. *Nat. Rev. Neurosci.* **13**, 107–120 (2012).
3. Kepecs, A. & Fishell, G. Interneuron cell types are fit to function. *Nature* **505**, 318–326 (2014).
4. Taniguchi, H. *et al.* A resource of Cre driver lines for genetic targeting of gabaergic neurons in cerebral cortex. *Neuron* **71**, 995–1013 (2011).
5. Nathanson, J.L., Yanagawa, Y., Obata, K. & Callaway, E.M. Preferential labeling of inhibitory and excitatory cortical neurons by endogenous tropism of adeno-associated virus and lentivirus vectors. *Neuroscience* **161**, 441–450 (2009).
6. Han, X. *et al.* Millisecond-timescale optical control of neural dynamics in the nonhuman primate brain. *Neuron* **62**, 191–198 (2009).
7. Nassi, J.J., Avery, M.C., Cetin, A.H., Roe, A.W. & Reynolds, J.H. Optogenetic activation of normalization in alert macaque visual cortex. *Neuron* **86**, 1504–1517 (2015).
8. Kotterman, M.A. & Schaffer, D.V. Engineering adeno-associated viruses for clinical gene therapy. *Nat. Rev. Genet.* **15**, 445–451 (2014).
9. Delzor, A. *et al.* Restricted transgene expression in the brain with cell-type specific neuronal promoters. *Hum. Gene Ther. Methods* **23**, 242–254 (2012).
10. Chen, Y.J. *et al.* Use of "MGE enhancers" for labeling and selection of embryonic stem cell-derived medial ganglionic eminence (MGE) progenitors and neurons. *PLoS One* **8**, e61956 (2013).
11. Marik, S.A., Yamahachi, H., McManus, J.N., Szabo, G. & Gilbert, C.D. Axonal dynamics of excitatory and inhibitory neurons in somatosensory cortex. *PLoS Biol.* **8**, e1000395 (2010).
12. Nathanson, J.L., Yanagawa, Y., Obata, K. & Callaway, E.M. Preferential labeling of inhibitory and excitatory cortical neurons by endogenous tropism of adeno-associated virus and lentivirus vectors. *Neuroscience* **161**, 441–450 (2009).

13. Dittgen, T. *et al.* Lentivirus-based genetic manipulations of cortical neurons and their optical and electrophysiological monitoring in vivo. *Proc. Natl. Acad. Sci. USA* **101**, 18206–18211 (2004).
14. Kügler, S., Kilic, E. & Bähr, M. Human *synapsin 1* gene promoter confers highly neuron-specific long-term transgene expression from an adenoviral vector in the adult rat brain depending on the transduced area. *Gene Ther.* **10**, 337–347 (2003).
15. Wu, Z., Yang, H. & Colosi, P. Effect of genome size on AAV vector packaging. *Mol. Ther.* **18**, 80–86 (2010).
16. Choi, J.-H. *et al.* Optimization of AAV expression cassettes to improve packaging capacity and transgene expression in neurons. *Mol. Brain* **7**, 17 (2014).
17. Zerucha, T. *et al.* A highly conserved enhancer in the *Dlx5/Dlx6* intergenic region is the site of cross-regulatory interactions between *Dlx* genes in the embryonic forebrain. *J. Neurosci.* **20**, 709–721 (2000).
18. Ghanem, N., Yu, M., Poitras, L., Rubenstein, J.L.R. & Ekker, M. Characterization of a distinct subpopulation of striatal projection neurons expressing the *Dlx* genes in the basal ganglia through the activity of the I56ii enhancer. *Dev. Biol.* **322**, 415–424 (2008).
19. Visel, A. *et al.* A high-resolution enhancer atlas of the developing telencephalon. *Cell* **152**, 895–908 (2013).
20. Ghanem, N. *et al.* Regulatory roles of conserved intergenic domains in vertebrate *Dlx* bigene clusters. *Genome Res.* **13**, 533–543 (2003).
21. Stühmer, T., Puelles, L., Ekker, M. & Rubenstein, J.L.R. Expression from a *Dlx* gene enhancer marks adult mouse cortical GABAergic neurons. *Cereb. Cortex* **12**, 75–85 (2002).
22. Stenman, J., Toresson, H. & Campbell, K. Identification of two distinct progenitor populations in the lateral ganglionic eminence: implications for striatal and olfactory bulb neurogenesis. *J. Neurosci.* **23**, 167–174 (2003).
23. Monory, K. *et al.* The endocannabinoid system controls key epileptogenic circuits in the hippocampus. *Neuron* **51**, 455–466 (2006).
24. Miyoshi, G. *et al.* Genetic fate mapping reveals that the caudal ganglionic eminence produces a large and diverse population of superficial cortical interneurons. *J. Neurosci.* **30**, 1582–1594 (2010).
25. Cobos, I., Long, J.E., Thwin, M.T. & Rubenstein, J.L. Cellular patterns of transcription factor expression in developing cortical interneurons. *Cereb. Cortex* **16** (Suppl. 1), i82–i88 (2006).
26. Xu, X., Roby, K.D. & Callaway, E.M. Mouse cortical inhibitory neuron type that coexpresses somatostatin and calretinin. *J. Comp. Neurol.* **499**, 144–160 (2006).
27. Punnakkal, P., von Schoultz, C., Haenraets, K., Wildner, H. & Zeilhofer, H.U. Morphological, biophysical and synaptic properties of glutamatergic neurons of the mouse spinal dorsal horn. *J. Physiol. (Lond.)* **592**, 759–776 (2014).
28. Fenno, L.E. *et al.* Targeting cells with single vectors using multiple-feature Boolean logic. *Nat. Methods* **11**, 763–772 (2014).
29. Roth, B.L. DREADDs for Neuroscientists. *Neuron* **89**, 683–694 (2016).
30. Armbruster, B.N., Li, X., Pausch, M.H., Herlitze, S. & Roth, B.L. Evolving the lock to fit the key to create a family of G protein-coupled receptors potently activated by an inert ligand. *Proc. Natl. Acad. Sci. USA* **104**, 5163–5168 (2007).
31. Alexander, G.M. *et al.* Remote control of neuronal activity in transgenic mice expressing evolved G protein-coupled receptors. *Neuron* **63**, 27–39 (2009).
32. Zou, D. *et al.* DREADD in parvalbumin interneurons of the dentate gyrus modulates anxiety, social interaction and memory extinction. *Curr. Mol. Med.* **16**, 91–102 (2016).
33. Urban, D.J. & Roth, B.L. DREADDs (designer receptors exclusively activated by designer drugs): chemogenetic tools with therapeutic utility. *Annu. Rev. Pharmacol. Toxicol.* **55**, 399–417 (2015).
34. Nord, A.S., Pattabiraman, K., Visel, A. & Rubenstein, J.L.R. Genomic perspectives of transcriptional regulation in forebrain development. *Neuron* **85**, 27–47 (2015).
35. Krook-Magnuson, E., Armstrong, C., Oijala, M. & Soltesz, I. On-demand optogenetic control of spontaneous seizures in temporal lobe epilepsy. *Nat. Commun.* **4**, 1376 (2013).
36. Kätzel, D., Nicholson, E., Schorge, S., Walker, M.C. & Kullmann, D.M. Chemical-genetic attenuation of focal neocortical seizures. *Nat. Commun.* **5**, 3847 (2014).
37. Whalen, S., Truty, R.M. & Pollard, K.S. Enhancer-promoter interactions are encoded by complex genomic signatures on looping chromatin. *Nat. Genet.* **48**, 488–496 (2016).

ONLINE METHODS

Animals. Female C57BL/6J mice (*Mus musculus*; 10 weeks old) were obtained from Taconic (New York, NY). Adult male zebra finches (*Taeniopygia guttata*; 90 d after hatching) were obtained from an outside breeder and maintained in a temperature- and humidity-controlled environment with a 12/12-h light/dark schedule. Adult gerbils (*Meriones unguiculatus*; 85 to 95 d old) were obtained from breeding pairs from Charles River Laboratories (Cambridge, MA). Juvenile female ferrets (*Mustela putorius furo*; postnatal d 27–30) were obtained from Marshall Farms. For mice, zebra finches and ferrets, all animal maintenance and experimental procedures were performed according to the guidelines established by the Institutional Animal Care and Use Committee at the New York University Langone Medical Center. All procedures were approved by the Max Planck Florida Institute for Neuroscience Institutional Animal Care and Use Committee. One female marmoset (*Callithrix jaccus*; 4.3 years old) was obtained from the University of Utah. All procedures were approved by the Salk Institute for Biological Studies Institutional Animal Care and Use Committee. All procedures adhered to the standards of the National Institutes of Health. All the animals were maintained in a 12 light/12 dark cycle with a maximum of five animals per cage for mice and one animal per cage for all other species.

Surgery. Animals were anesthetized under isoflurane (1–3% in oxygen) and placed in a stereotactic head frame on a temperature-controlled heating pad. A craniotomy and a durotomy were performed above region of interest. The animals were injected with 50–500 nl of the indicated virus at a rate of 10–25 nl/min using a sharp glass pipette (25–35 mm in diameter), which was left in place for 5–15 min after the injection to minimize backflow. The craniotomy site was covered with sterile bone wax, the surgical opening was closed with Vetbond and the animals were returned to their home cages for at least 1 week. The injection sites were defined by the following coordinates:

- Mice: somatosensory cortex S1: 1.0 mm posterior, 3.0 mm lateral, 0.7 /0.4 mm ventral relative to bregma; hippocampus CA1: 1.6 mm posterior, 1.8 mm lateral, 1.2 mm ventral relative to bregma; striatum: 0.5 mm posterior, 2.0 mm lateral, 3.2 mm ventral relative to bregma;
- Zebra Finches: HVC: 0,2 mm anterior, 2.1/2.3/2.5 mm lateral, 0.4 mm ventral relative to the bifurcation of the sagittal sinus;
- Gerbils: auditory cortex A1: 3.0 mm anterior, 6.5 mm lateral, 0.3 mm ventral relative to lambda;
- Ferrets: visual cortex V1: 2.0 mm anterior, 7.5 mm lateral, 0.25/0.4 mm ventral relative to lambda; and
- Marmoset: visual cortex V1: 15 mm anterior, 5 mm lateral, 1 mm ventral relative to bregma.

For zebra finches, the craniotomy was covered with a silicone elastomer (Kwik-Cast; WPI). For the subset of animals used for *in vivo* recording, a thin cover glass (3 mm, #1 thickness, Warner Instruments) was affixed to the skull using cyanoacrylate to create a chronic optical window over HVC. For ferrets, the scalp was retracted and a custom titanium head plate adhered to the skull using C&B Metabond (Parkell). One cover glass (5 mm in diameter, #1.5 thickness, Electron Microscopy Sciences) was adhered to a custom titanium cannula using optical adhesive (Norland Products) and placed onto the brain to gently compress the underlying cortex and dampen biological motion during imaging. The cranial window was hermetically sealed using a stainless steel retaining ring (5/16" or 7.94 mm) internal retaining ring, McMaster-Carr), Kwik-Cast (World Precision Instruments) and Vetbond (3M). For marmosets, the craniotomy was covered with an artificial dura made from bovine cells and the bone flap was fixed in place using Vetbond (3M). Following placement of the bone flap, the skin was sutured closed.

rAAV cloning and production. Detailed maps, sequences and plasmids corresponding to the viral constructs were deposited at Addgene. To clone these constructs, the plasmid AAV-CaMKIIa-GCaMP6f-P2A-nls-dTomato (a gift from Dr. Jonathan Ting; Addgene plasmid # 51087) was used to create a backbone containing either the mDlx or the hDlx enhancer sequences. The mDlx enhancer sequence (530 bp) was amplified by PCR from mouse genomic DNA using the following primers:

5′-TATACACTCACAGTGGTTTGGC-3′ and 5′-CTTCCTACTGTGAA ACTTTGGG-3′.

The hDlx enhancer sequence (541 bp) was amplified by PCR from human genomic DNA using the following primers:

5′-TTCAGAATGTTATGCACTCACA-3′ and 5′-CCCAAAGTTTCACAG TAGGAAG-3′.

The enhancers, reporters and effectors detailed below were subcloned using the Gibson Cloning Assembly Kit (NEB-E5510S) following standard protocol. For rAAV-mDlx-GFP, we amplified the GFP coding sequence from the plasmid pNeuroD-ires-GFP[38] (a gift from Dr. Franck Polleux; Addgene plasmid # 61403). For rAAV-mDlx-Flex-GFP, we amplified the GFP coding sequence and synthetized the fragments containing the noncompatible *loxP* sites by primer annealing[39]. For rAAV-mDlx-GCaMP6f, we amplified the GCaMP6f coding sequence from the plasmid pGP-CMV-GCaMP6f[40] (a gift from Dr. Douglas Kim; Addgene plasmid # 40755). For rAAV-mDlx-ChR2, we amplified the ChR2 coding sequence from the plasmid pAAV-Ef1a-DIO hChR2(E123T/T159C)-EYFP[41] (a gift from Dr. Karl Deisseroth ; Addgene plasmid # 35509) fused with the mCherry coding sequence. For rAAV-hDlx-Gq-DREADD, we amplified the Gq-DREADD coding sequence from the plasmid pAAV-hSyn-DIO-hM3D(Gq)-mCherry[42] (a gift from Bryan Roth; Addgene plasmid # 44361) and a P2A-NLS-dTomato from the plasmid AAV-hSyn1-GCaMP6s-P2A-nls-dTomato (a gift from Jonathan Ting; Addgene plasmid # 51084). The rAAVs were produced using standard production methods. PEI was used for transfection and OptiPrep gradient (Sigma, USA) was used for viral particle purification. Titer was estimated by qPCR with primers for the WPRE sequence that is common to all constructs. All batches produced were in the range of 10^{10} to 10^{12} viral genomes per ml.

Primary culture. Primary dissociated cortical neurons were prepared from C57BL/6J mice at postnatal day 0 (P0) using a previously described protocol[43]. Dissociated neurons were plated onto coverslips precoated with polyethyleneimine (0.1%; Sigma, USA) plus laminin (20 µg/ml; Life Technologies, USA) at a density of 3,000 cells/mm^2. The cultures were treated with AraC (1 µg/ml; Sigma, USA) on DIV 5 and maintained for up to 21 d after plating. All primary cultures were tested for mycoplasma contamination using standard protocol.

iPSCs derived neuronal culture. The iPSC line iPSC49026 was generated at the NYSCF Research Institute by mRNA/miRNA reprogramming technology from skin fibroblasts of a deidentified male healthy donor[44]. The skin biopsy was obtained after institutional review board approval and receipt of informed consent. iPSCs were maintained in feeder-free conditions, seeded onto Matrigel-coated plates (BD Biosciences) in the presence of mTeSR1 medium (StemCell Technologies). The iPSC-derived neurons were generated using the Livesey protocol[45] with minor modifications: the protocol was followed exactly up to the differentiation step where BrainPhys medium was used with 1 µM dbcAMP, 40 ng/ml BDNF, 40 ng/ml GDNF and 1 µg/ml Laminin. At 50 DIV, the cells were inoculated with rAAV-mDlx-GFP at a MOI of ~150K vg/cell and fixed with 4% PFA at 60 DIV. All iPSC cultures were tested for mycoplasma contamination using standard protocol.

hESCs derived neuronal culture. Lhx6-Citrine GABAergic interneurons were differentiated from an Lhx6-Citrine H9-reporter hESC line using a protocol as previously described[46]. Human excitatory neurons were obtained by forced expression of Ngn2 in a human iPSC line. At DIV 0, 200,000 hESC-Lhx6-Citrine interneurons and 200,000 Ngn2-induced excitatory neurons were plated on rat cortical feeders in a single 24-well. At DIV 1, the coculture was inoculated with rAAV-hDlx-Gq-DREADD at a MOI of 100,000 vg/cell and fixed at DIV 21. All cells were manipulated and cultured in a sterile environment using good cell culture practice and tested for mycoplasma using standard methods. All hESCs cultures were tested for mycoplasma contamination using standard protocol.

Electrophysiological recordings in mice. *Slice preparation.* Virally injected mice were anesthetized with intraperitoneal injection of pentobarbital (100 mg/kg body weight). Upon loss of reflexes, mice were transcardially perfused with ice-cold oxygenated ACSF containing the following (in mM): 87 NaCl, 75 sucrose, 2.5 KCl, 1.25 NaH_2PO_4, 26 $NaHCO_3$, 10 glucose, 1 $CaCl_2$ and 2 $MgCl_2$. Mice were then decapitated and 300-µm thick coronal slices were sectioned using a Leica VT-1200-S vibratome and incubated in a holding chamber at 32–35 °C for

doi:10.1038/nn.4430

15–30 min followed by continued incubation at room temperature 20–23.5 °C (68–74 °F) for at least 45–60 min before physiological recordings. Slice containing the injection site were transferred in a recording chamber submerged with oxygenated ACSF containing the following (in mM): 125 NaCl, 2.5 KCl, 1.25 NaH_2PO_4, 26 $NaHCO_3$, 10 glucose, 2 $CaCl_2$ and 1 $MgCl_2$ (pH = 7.4, bubbled with 95% O2 and 5% CO2).

Current clamp. For interneuron recording, 10 μM CNQX, 25 μM AP-5 and 10 μM SR-95531 were also added to block AMPA, NMDA and $GABA_A$ receptors, respectively, to measure the cell-intrinsic effect of CNO application. Whole-cell current-clamp recordings were obtained from visually identified dTomato expressing cells using borosilicate pipettes (3–5 MΩ) containing (in mM): 130 K-gluconate, 6.3 KCl, 0.5 EGTA, 10 HEPES, 4 Mg-ATP, 0.3 Na-GTP and 0.3% biocytin (pH adjusted to 7.3 with KOH). Upon break-in, series resistance (typically 15–25 MΩ) was compensated and only stable recordings (<20% change) were included. Data were acquired using a MultiClamp 700B amplifier (Molecular Devices), sampled at 20 kHz and filtered at 10 kHz. All cells were held at −60 mV with a DC current, and current-step protocols were applied to obtain firing patterns and to extract basic sub- and suprathreshold electrophysiological properties.

Voltage clamp. dTomato-negative cells were selected according to their pyramidal-cell-shaped soma under IR-DIC visualization and recorded with pipettes containing (in mM): 130 Cs-gluconate, 0.5 EGTA, 7 KCl, 10 HEPES, 4 Mg-ATP, 0.3 Na-GTP, 5 phosphocreatine, 5 QX-314 and 0.3% biocytin (pH adjusted to 7.3 with CsOH). Cells were held continuously at 0 mV for baseline and CNO application. For both current and voltage clamp recording, a baseline of at least 2 min was recorded before CNO (500 nM) was bath applied for at least 5 min. Small pulses (−20 pA or −5 mV, 100 ms at 0.2 Hz or 0.5 Hz) were applied throughout the baseline and CNO application to monitor series resistance changes. Data were analyzed offline using Clampfit 10.2 software (Molecular Devises).

Morphological identification. To confirm the morphology of recorded cells, slices were fixed for 1 h in 4% PFA following the recording and then in 30% sucrose for storage. For biocytin staining, slices were washed with PBS and incubated with streptavidin-conjugated Alexa Fluor (1:500) and 0.3% Triton X-100 in PBS overnight. Slices were then washed with PBS and mounted on microscope slides. Confocal image stacks were acquired using a Zeiss LSM510 microscope with a 20× objective.

Electrophysiological recordings in zebra finches. *Slice preparation.* All extracellular solutions were adjusted to 310 mOsm, pH 7.3–7.4, and aerated with a 95%/5% O_2/CO_2 mix. Zebra finches were first deeply anesthetized with an intramuscular injection of pentobarbital (40 mg/kg in saline). Once the animal was no longer responsive to a toe pinch, it was quickly decapitated, and the brain was removed from the skull and submerged in cold (1–4 °C) oxygenated zero-sodium ACSF containing the following (in mM): 225 sucrose, 3 KCl, 1.25 NaH_2PO_4, 26 $NaHCO_3$, 10 D-(+)-glucose, 2 $MgSO_4$, 2 $CaCl_2$. The brain was then cut along the sagittal plane and the medial side of the right hemisphere was glued onto a custom-made slice block. The block was constructed such that the vibratome blade entered the brain posteriorly at a 12° angle of elevation with respect to the glued medial side. Slices (300 m) containing HVC were produced using a vibratome (VT1200S; Leica) outfitted with a ceramic blade (Cadence) and an advancing speed of 0.12 mm/s. After cutting, slices were transferred to a recovery chamber at a temperature of 32 °C for 25 min with reduced sodium ACSF containing the following (in mM): 60 NaCl, 75 sucrose, 2.5 KCl, 1.2 NaH_2PO_4, 30 $NaHCO_3$, 25 D-(+)-glucose, 20 HEPES, 2 $MgSO_4$ and 2 $CaCl_2$. The slices remained in the recovery chamber for at least another 40 min at room temperature (23 °C) before electrophysiological recording.

Current-clamp recording. Whole-cell current-clamp recordings were obtained from visually identified GFP-expressing cells using borosilicate pipettes (3–5 MΩ) containing (in mM): 0.2 EGTA, 130 K-gluconate, 4 KCl, 2 NaCl, 10 HEPES, 4 ATP-Mg, 0.3 GTP-Tris, 14 phosphocreatine-Tris, 0.3% biocytin and brought to pH 7.25 and 292 mOsm. Upon break-in, series resistance (typically 15–25 MΩ) was compensated and only stable recordings (<20% change) were included. Data were acquired using a MultiClamp 700B amplifier, sampled at 20 kHz and filtered at 10 kHz. Current steps protocols were applied to obtain the firing pattern and to extract basic sub- and suprathreshold electrophysiological properties. Neuronal cell bodies were visualized for recording using an Axio Examiner A1 (Zeiss) fixed-stage upright microscope using IR-Dodt illumination through a 40× water-immersion objective. GFP positive neurons were targeted under visual-guidance fluorescing in the free wavelength using an Axiocam MRm fluorescence camera (Zeiss).

Morphological identification. To confirm the morphology of recorded cells, slices were fixed for 1 h in 4% PFA following the recording and then in 30% sucrose for storage. For biocytin staining, slices were washed with PBS and incubated with streptavidin-conjugated Alexa Fluor (1:500) and 0.3% Triton X-100 in PBS overnight. Slices were then washed with PBS and mounted on microscope slides. Confocal image stacks were acquired using a Zeiss LSM510 microscope with a 20× objective.

Two-photon targeted whole-cell recordings. On the day of recording, a small hole (~100 μm in diameter) was carefully drilled into the implanted cover slip using a carbide bur (0.3 mm in diameter) just lateral to the visually determined center of HVC and the recording was performed as previously described[47].

Optogenetics and electrophysiological recordings in gerbils. *Slice preparation.* Thalamo-cortical brain slices (500 μm thick) were prepared as previously described[48].

Current clamp recording. The ACSF contained (in mM): 125 NaCl, 4 KCl, 1.2 KH_2PO_4, 1.3 $MgSO_4$, 24 $NaHCO_3$, 15 glucose, 2.4 $CaCl_2$, and 0.4 L-ascorbic acid and bubbled with 95%O_2–5%CO_2 (pH 7.3). Before each whole-cell recording, the auditory cortex was identified by extracellular field responses evoked by stimulation of the auditory thalamus (Medial Geniculate Nucleus).

Whole-cell current-clamp optogenetic recording. Current-clamp recordings were obtained from pyramidal, fast-spiking and low-threshold-spiking neurons in L2/3 of the ACx. Each neuron was verified as thalamo-recipient by recording an MG-evoked response, and all data were collected within layer 2/3. The internal recording solution contained (in mM): 5 KCl, 127.5 K-gluconate, 10 HEPES, 2 $MgCl_2$, 0.6 EGTA, 2 ATP, 0.3 GTP and 5 phosphocreatine (pH 7.2 with KOH). The tip resistance of the patch electrode filled with internal solution was 5–10 MΩ. Access resistance was 15–30 MΩ and was compensated by ~70%. All data were acquired at a sampling rate of 10 kHz using a custom-designed IGOR (version 4.08; WaveMetrics, Lake Oswego, OR) macro on an iMac (Apple, Cupertino, CA). A second IGOR macro was used for offline analysis. Firing profiles were evaluated on the basis of responses to positive current pulses (1,500 ms) of 400 to 600 pA. For pyramidal neurons, inhibitory postsynaptic potentials (IPSPs) were evoked by passing positive current (400 to 600 pA) for 1.5 s coupled with 1 ms of blue light (20% intensity, 470 nm, lumen 1,600-lumen LED: Olympus) at 500 ms. Putative inhibitory cells (fluorescing) were patched using IR-IDC and mCherry filters. Threshold to action potential was achieved by gradually increasing light (470 nm) exposure (1 ms) from 0 to 20% intensity. Input–output functions were gathered by exposing the cell to increasing intensity of light (470 nm) exposure (1 ms) from 0 to 100% in 10% steps. All neuronal images were collected *in vitro* with a fluorescent camera (QImaging) equipped with an mCherry filter cube (Olympus) using QCapture Pro (QImaging).

Calcium imaging in mouse primary culture and in ferrets. GCaMP6f imaging were performed as previously described[43,49]. For primary culture, rAAV-mDlx-GCaMP6f (titer was 1×10^{12} vg/ml, 1 μl per well in 24-well plate) was added to neuronal cultures at DIV 8, and GCaMP imaging was performed 11 d after infection.

Immunohistochemistry. Citations with validation data for each antibody are reported on the providers' websites. For primary culture of mice neurons, iPSC-derived neuronal cultures and hESC-derived neuronal culture, neurons were fixed by incubation with 4% paraformaldehyde and 4% sucrose in phosphate-buffered saline (PBS) at room temperature for 5 min and then washed three times with PBS. Fixed neurons were permeabilized with 0.1% Triton X-100/PBS for 5 min, washed three times with PBS, and incubated in blocking buffer (3% bovine serum albumin plus 10% normal goat serum in PBS) for 1 h. The cells were then incubated overnight in blocking buffer with the indicated combination of the following primary antibodies at 4 °C: rabbit anti-GFP at 1:1,000 (Invitrogen, A6455, USA); mouse anti-GAD67 at 1:1,000 (Millipore, 1G10.2, USA); mouse anti-Stem-121 (Clontech, Y40410, USA); mouse anti-GABA at 1:1,000 (Sigma, A0310, USA). The cells were then washed three times with PBS and incubated with Alexa conjugated secondary antibodies (Invitrogen, USA). Animals injected with the virus were euthanized with Euthasol (Virbac, USA)

and transcardially perfused with 4% paraformaldehyde (PFA). The brains were placed in 4% PFA overnight then sectioned at 50–60 μm using a Leica VTS1000 vibrosector. Floating sections were permeabilized with 0.1% Triton X-100 and PBS for 30 min, washed three times with PBS and incubated in blocking buffer (3% bovine serum albumin plus 5% normal goat serum plus 5% normal donkey serum in PBS) for 1 h. The sections were then incubated overnight in blocking buffer with the indicated combination of the following primary antibodies at 4 °C: chicken anti-GFP at 1:1,000 (Abcam, ab13970, USA); rabbit anti-GABA at 1:500 (Sigma, A2052, USA); rabbit anti-DsRed at 1:1,000 (Clontech, 632496, USA); rabbit anti-Nkx2.1 at 1:2,000 (Abcam, ab76013, USA); goat anti-PV at 1:1,000 (Swant, PVG-213, USA); rat anti-SST at 1:400 (Millipore, MAB354, USA); rabbit anti-VIP at 1:500 (Immunostar, 20077, USA); goat anti-HA at 1:1,000 (Abcam, ab9134, USA) and rabbit anti-GAD65/67 at 1:1,000 (Abcam, ab11070, USA) for ferret. P7 spinal cord preparations were fixed by incubation with 4% paraformaldehyde and incubated overnight in 4% sucrose in phosphate-buffered saline (PBS), then washed three times with PBS and cryosectioned at 30 μm. Cryosections were incubated in blocking buffer (3% bovine serum albumin plus 10% normal goat serum in PBS) for 1 h and then incubated overnight in blocking buffer with the indicated combination of the following primary antibodies at 4 °C: chicken anti-GFP at 1:1,000 (Invitrogen,A10262, USA) and rabbit anti-Pax2 1:500 (Invitrogen, 71-6000, USA). The sections were then washed three times with PBS, incubated with Alexa Fluor-conjugated secondary antibodies at 1:500 (Invitrogen, USA), counterstained with DAPI (Sigma, USA) and mounted on glass slides using Fluoromount-G (Sigma, USA). Note that for mouse and marmoset immunostaining for Gad67, mouse anti-GAD67 at 1:200 (Millipore, MAB506, USA) was incubated at room temperature for 48 h. Incubation of primary, secondary and intermediate washes were performed in 0.1 M PBS without detergent. Confocal images were acquired using a Zeiss LSM510 and LSM800 confocal microscopes.

Quantification and statistics. For quantification of colocalization, cells expressing the indicated reporter were counted using only the corresponding color channel, and then among these cells, the number of cells coexpressing the marker of interest were counted. A cell was considered to be positive for a given marker if the corresponding signal was significantly above background fluorescence. For animals, the brain sections containing the highest number of cells expressing the viral reporter were used for quantification. Several sections from the same animal were used when indicated. For *in vitro* studies, all the cells from randomly selected fields were counted. Data collection and analysis were not performed blind to the conditions of the experiments, but experimenters from different research groups performed the quantification. The ratio of cells coexpressing both markers over the total number of cells expressing only the reporter was then calculated, reported here as mean ± s.e.m. and represented in figures as box-and-whisker plots with upper and lower whiskers representing the maximum and minimum values, respectively, and boxes representing the upper, median and lower quartiles. Quantifications were performed using a minimum of two independent biological replicates (the specific number of cells, animals and conditions are indicated for each individual quantification in the figure legends). An unpaired *t*-test was performed to estimate the statistical differences in the right and left panels of **Figure 3c** (equal variance between the two populations was not tested; df = 8 and 18, respectively). No statistical methods were used to predetermine sample sizes, but our sample sizes are similar to those reported in previous publications.

A **Supplementary Methods Checklist** is available.

Data availability statement. The data that support the findings of this study are available from the corresponding author upon reasonable request.

38. Guerrier, S. *et al.* The F-BAR domain of srGAP2 induces membrane protrusions required for neuronal migration and morphogenesis. *Cell* **138**, 990–1004 (2009).
39. Saunders, A., Johnson, C.A. & Sabatini, B.L. Novel recombinant adeno-associated viruses for Cre activated and inactivated transgene expression in neurons. *Front. Neural Circuits* **6**, 47 (2012).
40. Chen, T.-W. *et al.* Ultrasensitive fluorescent proteins for imaging neuronal activity. *Nature* **499**, 295–300 (2013).
41. Mattis, J. *et al.* Principles for applying optogenetic tools derived from direct comparative analysis of microbial opsins. *Nat. Methods* **9**, 159–172 (2011).
42. Krashes, M.J. *et al.* Rapid, reversible activation of AgRP neurons drives feeding behavior in mice. *J. Clin. Invest.* **121**, 1424–1428 (2011).
43. Lu, C. *et al.* Micro-electrode array recordings reveal reductions in both excitation and inhibition in cultured cortical neuron networks lacking Shank3. *Mol. Psychiatry* **21**, 159–168 (2016).
44. Paull, D. *et al.* Automated, high-throughput derivation, characterization and differentiation of induced pluripotent stem cells. *Nat. Methods* **12**, 885–892 (2015).
45. Shi, Y., Kirwan, P. & Livesey, F.J. Directed differentiation of human pluripotent stem cells to cerebral cortex neurons and neural networks. *Nat. Protoc.* **7**, 1836–1846 (2012).
46. Maroof, A.M. *et al.* Directed differentiation and functional maturation of cortical interneurons from human embryonic stem cells. *Cell Stem Cell* **12**, 559–572 (2013).
47. Vallentin, D., Kosche, G., Lipkind, D. & Long, M.A. Neural circuits. Inhibition protects acquired song segments during vocal learning in zebra finches. *Science* **351**, 267–271 (2016).
48. Kotak, V.C. *et al.* Hearing loss raises excitability in the auditory cortex. *J. Neurosci.* **25**, 3908–3918 (2005).
49. Chen, Q. *et al.* Imaging neural activity using *Thy1-GCaMP* transgenic mice. *Neuron* **76**, 297–308 (2012).

doi:10.1038/nn.4430

Corrigendum: A viral strategy for targeting and manipulating interneurons across vertebrate species

Jordane Dimidschstein, Qian Chen, Robin Tremblay, Stephanie L Rogers, Giuseppe-Antonio Saldi, Lihua Guo, Qing Xu, Runpeng Liu, Congyi Lu, Jianhua Chu, Michael C Avery, Mohammad S Rashid, Myungin Baek, Amanda L Jacob, Gordon B Smith, Daniel E Wilson, Georg Kosche, Illya Kruglikov, Tomasz Rusielewicz, Vibhakar C Kotak, Todd M Mowery, Stewart A Anderson, Edward M Callaway, Jeremy S Dasen, David Fitzpatrick, Valentina Fossati, Michael A Long, Scott Noggle, John H Reynolds, Dan H Sanes, Bernardo Rudy, Guoping Feng & Gord Fishell

Nat. Neurosci. **19, 1743–1749 (2016); published online 31 October 2016; corrected after print 29 November 2016**

In the version of this article initially published, authors Joshua S. Grimley, Anne-Rachel Krostag and Ajamete Kaykas were missing. These authors have been inserted into the author list after Jianhua Chu; they are at the Allen Institute for Brain Science, Seattle, Washington, USA, and performed experiments related to hESCs. The error has been corrected in the HTML and PDF versions of the article.

Addendum: A viral strategy for targeting and manipulating interneurons across vertebrate species

Jordane Dimidschstein, Qian Chen, Robin Tremblay, Stephanie L Rogers, Giuseppe-Antonio Saldi, Lihua Guo, Qing Xu, Runpeng Liu, Congyi Lu, Jianhua Chu, Michael C Avery, Mohammad S Rashid, Myungin Baek, Amanda L Jacob, Gordon B Smith, Daniel E Wilson, Georg Kosche, Illya Kruglikov, Tomasz Rusielewicz, Vibhakar C Kotak, Todd M Mowery, Stewart A Anderson, Edward M Callaway, Jeremy S Dasen, David Fitzpatrick, Valentina Fossati, Michael A Long, Scott Noggle, John H Reynolds, Dan H Sanes, Bernardo Rudy, Guoping Feng & Gord Fishell

***Nat. Neurosci.* 19, 1743–1749 (2016); published online 31 October 2016; corrected after print 29 November 2016; addendum published after print 29 May 2017**

The authors wish to acknowledge a potentially relevant work that they were made aware of after publication: Lee, A.T., Vogt, D., Rubenstein, J.L. & Sohal, V.S. A class of GABAergic neurons in the prefrontal cortex sends long-range projections to the nucleus accumbens and elicits acute avoidance behavior. *J. Neurosci.* **34**, 11519–11525, http://dx.doi.org/10.1523/JNEUROSCI.1157-14.2014 (2014). This work describes an approach for using Dlx1/2 enhancers to attempt to achieve selective expression in cortical GABAergic interneurons. Although thorough validation was not performed, the results are consistent with the possibility that other regulatory elements may be generalizable as an effective way of targeting specific cell types.